Perivascular Macrophages Limit Permeability

Huanhuan He, Julia J. Mack, Esra Güç, Carmen M. Warren, Mario Leonardo Squadrito, Witold W. Kilarski, Caroline Baer, Ryan D. Freshman, Austin I. McDonald, Safiyyah Ziyad, Melody A. Swartz, Michele De Palma, M. Luisa Iruela-Arispe

Objective—Perivascular cells, including pericytes, macrophages, smooth muscle cells, and other specialized cell types, like podocytes, participate in various aspects of vascular function. However, aside from the well-established roles of smooth muscle cells and pericytes, the contributions of other vascular-associated cells are poorly understood. Our goal was to ascertain the function of perivascular macrophages in adult tissues under nonpathological conditions.

Approach and Results—We combined confocal microscopy, in vivo cell depletion, and in vitro assays to investigate the contribution of perivascular macrophages to vascular function. We found that resident perivascular macrophages are associated with capillaries at a frequency similar to that of pericytes. Macrophage depletion using either clodronate liposomes or antibodies unexpectedly resulted in hyperpermeability. This effect could be rescued when M2-like macrophages, but not M1-like macrophages or dendritic cells, were reconstituted in vivo, suggesting subtype-specific roles for macrophages in the regulation of vascular permeability. Furthermore, we found that permeability-promoting agents elicit motility and eventual dissociation of macrophages from the vasculature. Finally, in vitro assays showed that M2-like macrophages attenuate the phosphorylation of VE-cadherin upon exposure to permeability-promoting agents.

Conclusions—This study points to a direct contribution of macrophages to vessel barrier integrity and provides evidence that heterotypic cell interactions with the endothelium, in addition to those of pericytes, control vascular permeability. **(*Arterioscler Thromb Vasc Biol*. 2016;36:2203-2212. DOI: 10.1161/ATVBAHA.116.307592.)**

Key Words: capillaries ■ capillary permeability ■ cell communication ■ endothelial cells ■ macrophages

Macrophages are versatile cells that function as scavengers to eliminate cellular debris and contribute to the innate immune response. Some macrophages are short-lived, particularly those recruited during inflammation. In contrast, resident macrophages are long-lived, specialized cells that are part of almost every tissue and represent a phenotype wired for repair.[1,2] Importantly, macrophages also exist in different activation states, whose extremes are referred to as M1 and M2 in analogy to Th1 and Th2 T cells.[2]

See cover image

The cross talk between macrophages and the vasculature has been significantly explored in the context of cancer.[3–5] Perivascular M2-like macrophages play a crucial role in tumor angiogenesis, and depletion of these cells significantly interferes with neovascularization, tumor growth, and cancer progression.[6–9] In general, M2-like macrophages are considered to be proangiogenic, whereas M1-like macrophages may be angiostatic.[5] Using in vitro Matrigel angiogenesis assays, it has been shown that M2-like macrophages, and not M1-like macrophages, promote endothelial tube formation and colocalize with endothelial branch points.[10] These findings are consistent with the notion that during development, macrophages coordinate fusion of adjacent vascular sprouts, as they facilitate the bridging between filopodia and aid in vascular anastomosis.[11,12] Together, these functions portray macrophages as important regulators of angiogenesis.

Although well accepted, the M1 to M2 paradigm is probably oversimplified. There most likely exist a spectrum of macrophage phenotypes in between the well-characterized M1 to M2 poles. Heterogeneous mixtures of macrophages with diverse phenotypes populate specific microenvironments, and the makeup of these populations is highly dependent on local cytokines.[13] In fact, recent macrophage transcriptome analyses revealed functional polarization of macrophages based on tissue-specific influences.[14–17] These reports demonstrate the importance of environmental cues for functional polarization of macrophages. Moreover, macrophages have been described as controllers of tissue homeostasis that can sense and respond to environmental factors and perform accordingly.[18]

Received on: March 8, 2016; final version accepted on: August 31, 2016.

From the Department of Human Genetics (H.H.), Department of Molecular, Cell and Developmental Biology (J.J.M., C.M.W., R.D.F., A.I.M., S.Z., M.L.I.-A.), Molecular Biology Institute (M.L.I.-A.), and Jonsson Comprehensive Cancer Center (M.L.I.-A.), University of California, Los Angeles; Institute for Bioengineering (IBI) (E.G., M.A.S.) and The Swiss Institute for Experimental Cancer Research (ISREC) (M.L.S., C.B., M.A.S., M.D.P., M.L.I.-A.), School of Life Sciences, Ecole Polytechnique Fédérale de Lausanne, Switzerland; and Institute for Molecular Engineering and Ben May Department of Cancer Research, University of Chicago, IL (W.W.K., M.A.S.).

Current address for H.H.: Department of Cell, Developmental and Cancer Biology, Oregon Health and Science University, Mail Code L215, Portland, OR.

The online-only Data Supplement is available with this article at http://atvb.ahajournals.org/lookup/suppl/doi:10.1161/ATVBAHA.116.307592/-/DC1.

Correspondence to Luisa Iruela-Arispe, PhD, Department of Molecular, Cell and Developmental Biology, Biomedical Sciences, Room 447, UCLA, 615 Charles Young Dr S, Los Angeles, CA 90095. E-mail arispe@mcdb.ucla.edu

Nonstandard abbreviations and Acronyms	
ECs	endothelial cells
iBMMs	immortalized bone marrow macrophages

From previous work, we have shown that endothelial cells (ECs) provide a specific niche for the differentiation of macrophages in culture and that contact with the endothelium favors M2-polarization.[19] Even in the absence of vascular pathology in vivo, monocytes/macrophages have been shown to patrol the inner surface of the endothelial wall and, in some cases, associate externally with capillaries.[20] These observations beg the question of the role of these perivascular macrophages under homeostatic conditions.

Perivascular cells are known to play roles in capillary stability, protection against antiangiogenic drugs, and vascular constriction.[21] Pericytes are the prototypical and best studied perivascular cell type although smooth muscle cells, macrophages, and other tissue-specific cells such as podocytes and microglia are also included in this category. Their overlapping and distinctive functions, as well as tissue-specific contributions, are poorly understood.

In the current study, we sought to investigate the biological relevance of perivascular macrophages under homeostatic conditions. Real-time visualization of macrophage–endothelial interactions, as well as depletion and reconstitution of macrophages in vivo, revealed an unpredicted role for macrophages in the regulation of vascular barrier function.

Materials and Methods

Materials and Methods are available in the online-only Data Supplement.

Results

Frequent Association of Macrophages With Blood Vessels Under Nonpathological Conditions

Macrophages are common residents of tissues and can be found in the vicinity of most blood vessels. To better characterize the association between resident macrophages and small-caliber vessels, we examined the distribution of macrophages on mesenteric vessels by confocal microscopy. We selected the mesentery because of its accessibility and relative transparency. From 3-dimensional reconstruction of z-stack confocal images, we noted that macrophages were frequently associated with mesenteric vessels (Figure 1A; Figure IA and IB in the online-only Data Supplement). These macrophages were often located on the abluminal side of blood vessels but were also found juxtaposed to the lumen and actively crossing the endothelial wall (Figure IC in the online-only Data Supplement). Using macrophage and myeloid-specific markers (F4/80 and Mac1), we identified the population of perivascular macrophages located on the abluminal aspect of microvessels. This population comprised ≈20% of all cells in the mesentery (Figure 1B through 1E). The majority of these macrophages by flow cytometric analysis expressed the M2-like macrophage marker, Mrc1 (or CD206; Figures ID and IIA and IIB in the online-only Data Supplement). To be noted, the morphology and location of these macrophages were distinct from those of pericytes (Figure 1F and 1G) or smooth muscle cells (Figure IIC in the online-only Data Supplement). By intravital microscopy, we confirmed that this population of perivascular macrophages ($Mrc1^{+}$ cells) was also present in vessels of the dermis (Figure ID in the online-only Data Supplement, white arrowheads). Importantly, perivascular macrophages were morphologically elongated and characterized by $Mrc1^{high}$ $Mac1^{low}$, in contrast to $Mac1^{high}$ macrophages that were rounded and more broadly distributed in the tissue (Figure 1H; Figure IID in the online-only Data Supplement). These imaging experiments revealed that under nonpathological conditions, there was a direct and frequent association between macrophages and blood vessels. Furthermore, these perivascular macrophages expressed markers that indicated M2-polarity.

Resident Macrophages Contribute to the Regulation of the Endothelial Barrier

We next explored the biological relevance of the association between macrophages and blood vessels by removing macrophages in vivo and subsequently evaluating the effect of macrophage removal on vascular function in real time. Macrophages were depleted from the ear by intradermal clodronate liposome injection (Figure 2A), whereas the contralateral ear was injected with control (PBS-loaded) liposomes. Clodronate liposome treatment resulted in a 70% reduction of macrophages by flow cytometric analysis (Figure 2B). The marked depletion of macrophages was not associated with any obvious structural abnormalities in blood vessels, but caused a significant decrease in barrier integrity and a hyperpermeable vascular response in the absence of any permeability mediator (Figure 2C and 2E). These findings indicate that at baseline perivascular macrophages contribute to suppress permeability. To further examine whether these effects were in fact because of barrier dysfunction, we applied VEGFA (Vascular Endothelial Growth Factor A), a strong vascular permeability enhancer. Intravital imaging was initiated 5 minutes after VEGFA application and recorded for 20 minutes. Macrophage-depleted vasculature exhibited a striking elevation in vascular leakage on VEGFA exposure, whereas the control group showed only a modest increase in permeability by comparison (Figure 2D and 2F). Note that the vascular dilatation induced by VEGFA in both the control group and the clodronate-treated group was equivalent (Figure 2D). In fact, vascular diameter increased by 1.254% (±0.04%) in control and by 1.242% (±0.036%) on clodronate treatment in equivalent-sized vessels (n=6, data not shown), indicating that the vasodilation response was unaffected, but barrier integrity was compromised.

To verify that the macrophage-mediated permeability was not solely dependent on VEGFA, we tested another permeability factor, bradykinin. On bradykinin addition, macrophage-depleted vessels also displayed a greater increase in permeability compared with vehicle-exposed vessels although the change was less drastic than that induced by VEGFA exposure (Figure IIIA and IIIB in the online-only Data Supplement). This was not surprising because VEGF is

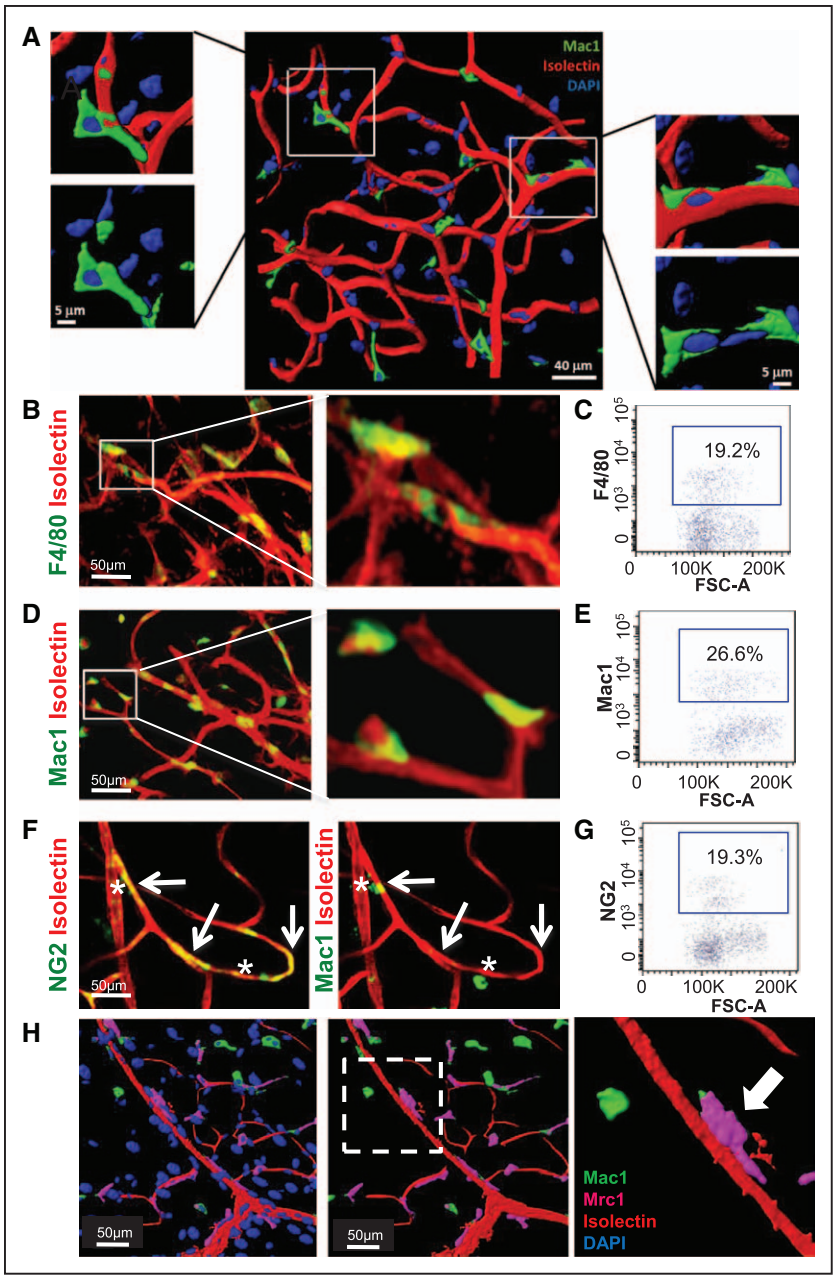

Figure 1. Frequent association of macrophages with blood vessels under non-pathological states. **A**, Three-dimensional reconstruction (magnified in boxes) of confocal z-stack reveals the association between macrophages and blood vessels. Mac1 labels macrophages (green). Isolectin labels vessels (red). DAPI (4′,6-diamidino-2-phenylindole) labels nuclei. Left magnified area shows an example of macrophages located on the abluminal side of blood vessels. Right magnified area shows an example of transvascular macrophages. **B**, **D**, and **F**, Maximum intensity projection of confocal z-stack of mesenteric fragments labeled by markers as indicated. **C**, **E**, and **G**, Representative flow cytometry plots of mesenteric fragments labeled by markers as indicated. **H**, Macrophages in close association with vessels express Mac1/CD11b or Mrc1/CD206 (purple).

the most potent inducer of vascular permeability and reported to be 50 000 × more potent than histamine or bradykinin.[22,23] Importantly, exposure to clodronate did not have an effect on the viability of ECs, pericytes, or smooth muscle (Figure IIIC in the online-only Data Supplement).

Next, we tested vascular permeability in *op/op* mice, which are deficient in Csf1–derived macrophages. The bone marrow resident macrophage populations in control versus *op/op* homozygous mice were characterized via flow cytometry to reveal a significant reduction in F4/80-positive cells in the total CD45$^+$ population (Figure IIID in the online-only Data Supplement). Confocal imaging demonstrated an absence of Mac1-stained macrophages in the mesentery and a disordered vascular architecture (Figure 2G). Baseline peritoneal permeability after intravenous fluorescein isothiocyanate-ovalbumin injection was higher in the *op/op* mice than in the controls (Figure 2H). This result provides further evidence that macrophages participate in regulating vascular permeability in vivo.

Reconstitution of Macrophages in the Peritoneum Rescues Vascular Permeability

To determine whether macrophages were primarily responsible for the changes in vascular permeability, we considered a rescue approach. Macrophages were depleted from the peritoneum by intraperitoneal injection of clodronate liposomes following the protocol shown in Figure 3A. Flow cytometric analysis confirmed a major reduction of macrophages in the peritoneal cavity (Figure 3B). Subsequently, we evaluated the effect of macrophage depletion on peritoneal permeability and detected a faster and greater vascular leakage compared with control (Figure 3C). To determine whether macrophages contributed to the observed differences in

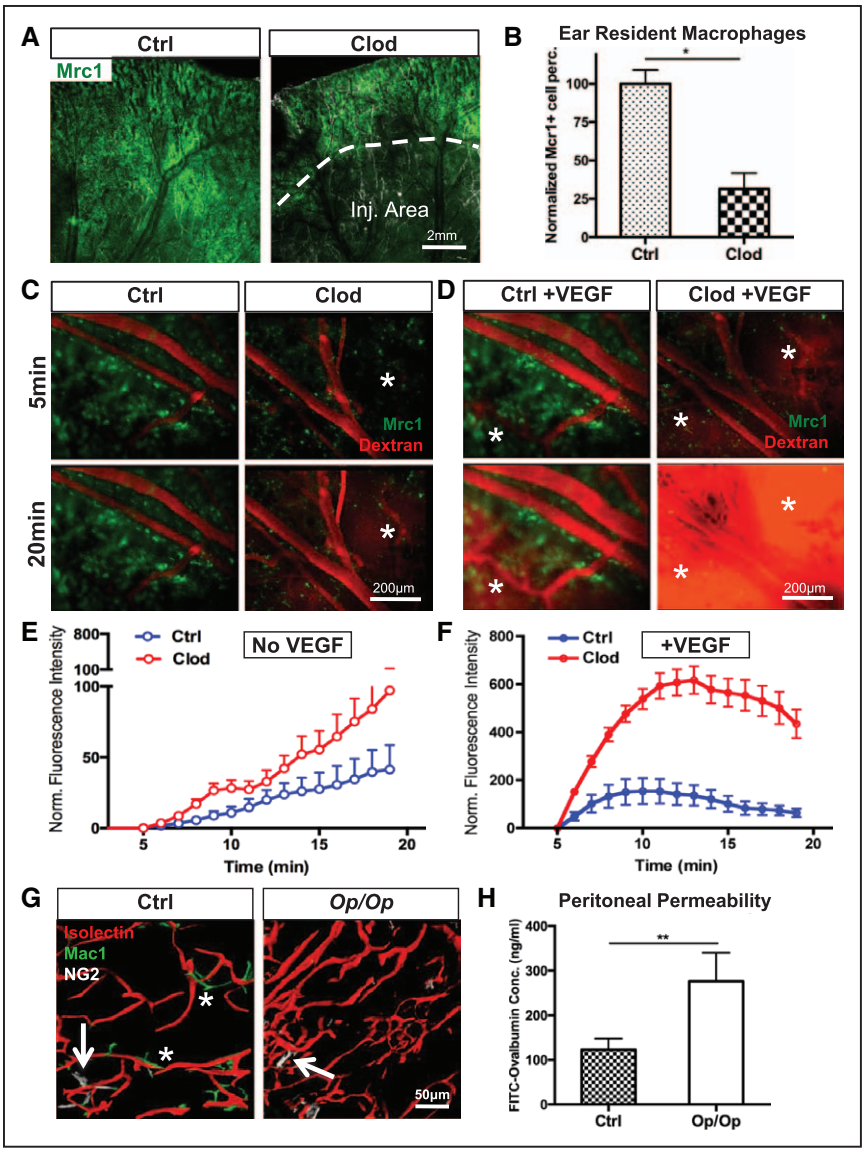

Figure 2. Resident macrophages contribute to the regulation of endothelial barrier. **A**, Macrophages (marked by Mrc1) were depleted by clodronate liposome (Clod) injection (dermis, ear). Ctrl, PBS-liposome. Dash line circles liposome injected area. **B**, Quantification of resident macrophages (Mrc1$^+$) on the ear by flow cytometric analysis. n=4 to 5. Statistics: Wilcoxon rank-sum test, P=0.0159. **C** and **D**, Micrographs from intravital imaging recording the tetramethylrhodamine isothiocyanate (TRITC)-Dextran leakage on the ear. Ears were injected with either clodronate liposomes (Clod) or PBS-liposomes (Ctrl) and injected intradermally with vehicle (**C**) or VEGFA (Vascular Endothelial Growth Factor A, 5 μg/mL; **D**). Note the permeability (indicated by star) and the decrease of Mrc1$^+$ cells on VEGFA treatment. **E** and **F**, Quantification of TRITC-Dextran in ears exposed to vehicle or VEGFA, n=3. **G** and **H**, Analysis of control and op/op mice. **G**, Three-dimensional reconstruction of mesentery segments stained for blood vessels (isolectin), pericytes (NG2), and macrophages (Mac1). **H**, Peritoneal permeability was assessed by leakage of fluorescein isothiocyanate-ovalbumin, n=7. Statistics: Wilcoxon rank-sum test, P=0.0022.

permeability, unpolarized macrophages derived from bone marrow were reintroduced via intravenous injection 2 days before measuring peritoneal permeability. A significant reduction of permeability (58%) was detected on the reconstitution of macrophages (Figure 3D). This indicates that in fact macrophages play an essential role in the regulation of vascular permeability.

Effect of Different Subtypes of Macrophages on Vascular Permeability

Although clodronate liposomes have been extensively used to deplete macrophages, we could only eliminate 70% of the population. Thus, we explored an alternative approach to eliminate macrophages and further expand our initial findings. Specifically, we used an antibody against CSF1R,[24] which exclusively blocks the CSF1 pathway necessary for macrophage survival (Figure 4A). After treatment with the antibody, peritoneal macrophages were reduced by ≈90%, a higher percentage than the clodronate effect (Figure 4B through 4D). Importantly, the antibody did not appear to have deleterious disruption in blood vessels (Figure 4C). Furthermore, the antibody did not affect barrier function in vitro (transendothelial resistance), or induced an inflammatory response in the endothelium alone (Figure IVA and IVB in the online-only Data Supplement).

After determining clearance of the antibody from the mouse circulation (by ELISA), we tested whether intravenous-injected macrophages could extravasate into the mesentery. To trace the injected cells, we used mCherry-labeled immortalized bone marrow macrophages (iBMMs, characterized in Figure VA and VB in the online-only Data Supplement) for quantifying extravasated peritoneal macrophages. Sixteen hours after intravenous injection, 37% mCherry-positive cells were detected in the peritoneal cavity, indicating the significant homing potential of macrophages to that site (Figure 4E and 4F).

To determine the role of different subtypes of macrophages in the control of permeability, we injected polarized M1-like iBMMs, M2-like iBMMs, or bone marrow–derived dendritic cells into macrophage-depleted animals. A detailed characterization of iBMMs before and after polarization of

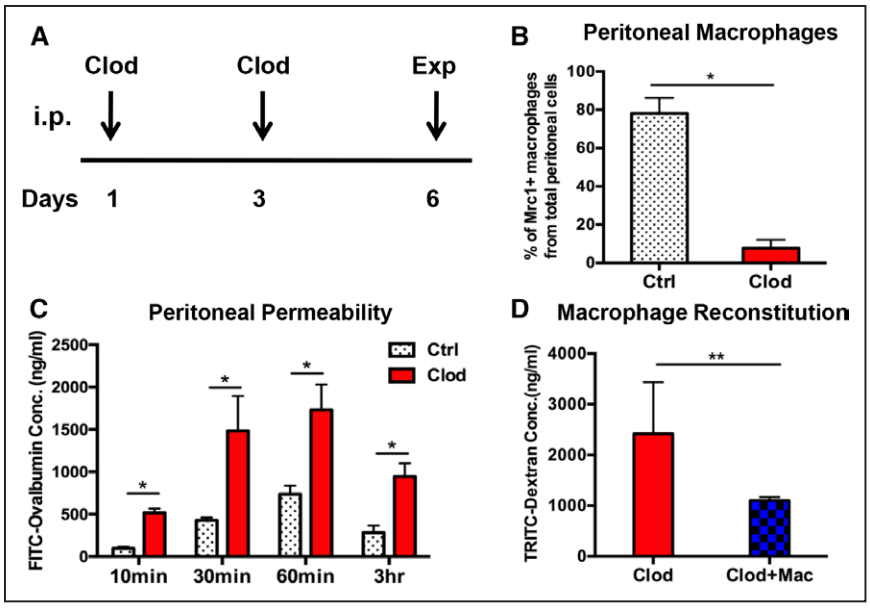

Figure 3. Reconstitution of macrophages in the peritoneum rescues vascular permeability. **A**, Schematic experimental design for the clodronate liposome injections. **B**, Peritoneal macrophages were quantified by flow cytometry using Mrc1 expression after injection of clodronate liposomes (Clod) or PBS-liposome (Ctrl), n=5. Statistics: Wilcoxon rank-sum test, P=0.0159. **C**, Kinetics of permeability were measured by fluorescein isothiocyanate-ovalbumin leakage into peritoneal cavity over time, n=5 for each time point. Statistics: Wilcoxon rank-sum test, P=0.0159 (for 10, 30, and 60 min), P=0.0286 (for 3 h). **D**, Evaluation of permeability after macrophage reconstitution (10^6 cells per animal) and measured by tetramethylrhodamine isothiocyanate-Dextran exit from the blood stream into the peritoneal cavity after 60 min. n=3 for control group, n=8 for injected macrophages. Statistics: Wilcoxon rank-sum test, P=0.0079. i.p. indicates intraperitoneal injection.

M1 and M2 is provided in Figure VC and VD in the online-only Data Supplement. Determination of peritoneal permeability showed that only M2-like macrophages rescued the vascular permeability, which points to the specific role of M2-like macrophages in the protection from vascular permeability (Figure 4G).

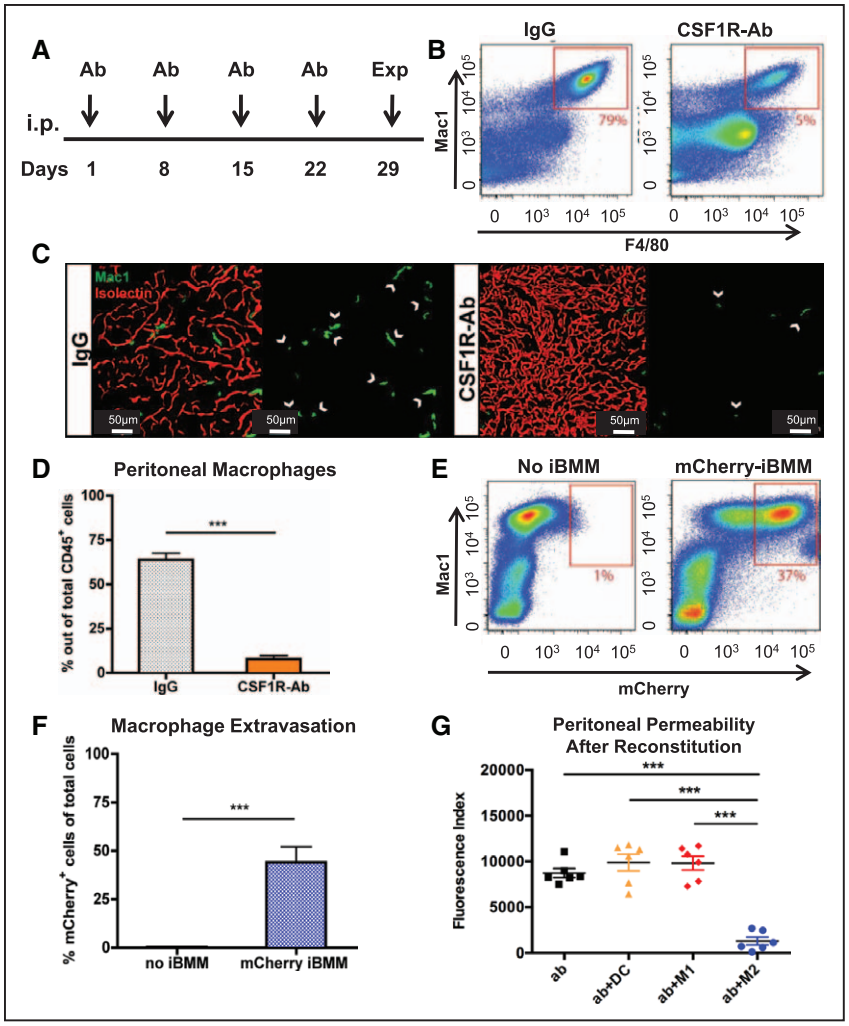

Figure 4. Effect of different subtypes of macrophages on vascular permeability. **A**, Schematic experimental design of anti-CSF1R antibody injection protocol. **B**, Peritoneal macrophages were depleted by anti-CSF1R antibody and efficiency of depletion was assessed by flow cytometry. **C**, Mesenteric vessels were stained with isolectin and imaged for Mac1 distribution. **D**, Quantification of peritoneal macrophages using control (IgG) or CSF1R antibodies. **E**, Extravasation of mCherry-labeled macrophages in the peritoneum 16 h after intravenous injection was evaluated by flow cytometry. **F**, Quantification of macrophage extravasation detected by mCherry expression. n=4 to 6. **G**, Peritoneal permeability 72 h after injection of indicated cells in the peritoneum. Ab indicates anti-CSF1R antibody; DCs, dendritic cells derived from bone marrow; Exp, evaluation of permeability; iBMM, immortal bone marrow macrophages; i.p., intraperitoneal injection; M1, bone marrow–derived macrophages activated by lipopolysaccharide (50 ng/mL). M2, bone marrow–derived macrophages activated by interleukin-4 (10 ng/mL). n=6 for each group. ***P<0.001 (unpaired Student t test for **D**, **F**; Tukey's multiple comparison for **G**).

Macrophage Motility Is Increased on Induction of Vascular Permeability

During intravital imaging, we observed an obvious increase in macrophage motility when permeability was induced (Figure 5A). We considered that this might be an important component of the permeability response. To verify and quantify this observation, we tracked macrophage motility at an individual cell level and the combined change in macrophage motility in a field of view over time when tissues were exposed to VEGFA or vehicle control. Individual macrophages (Figure 5B and 5D) were analyzed with a motility program as described in the Materials and Methods in the online-only Data Supplement. Briefly, the difference in pixel location between distinct time frames was determined by changes in area occupied by the cell and normalized to the average of the total area. The approach revealed pixels that were different between 2 consecutive frames and could be visualized by different colors. In this manner, we obtained a compressed readout of all

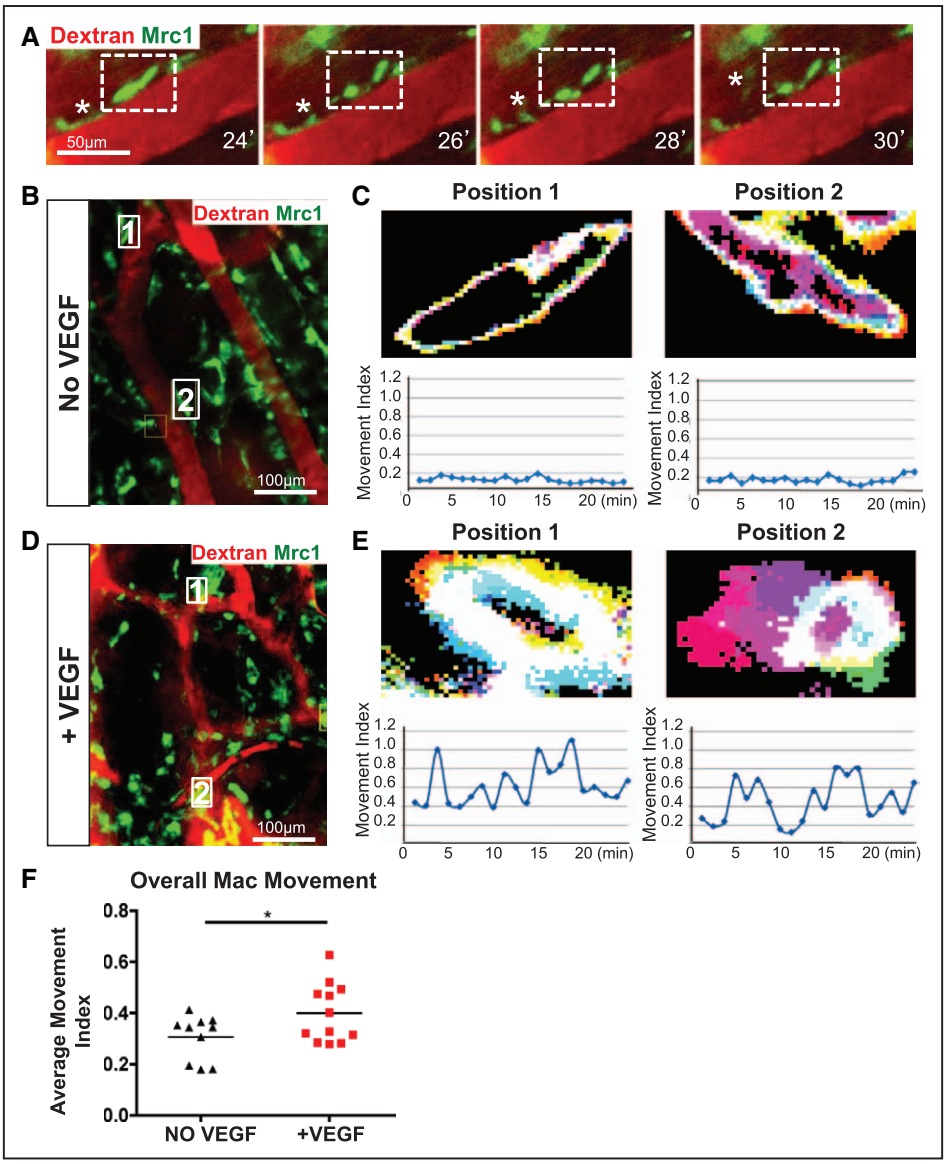

Figure 5. Macrophage motility is increased on induction of vascular permeability. **A**, Representative snapshots from intravital imaging of ear vessels exposed to VEGFA (Vascular Endothelial Growth Factor A). Two macrophages (in dashed box) were tracked and captured to detach from the vessel. The macrophage identified by * became completely dissociated from vessel wall over the time course of imaging. **B**, Snapshots from intravital imaging video of ear vessels without VEGFA treatment. Leakage was tracked after the injection of tetramethylrhodamine isothiocyanate-Dextran. Two individual cells are shown. **C**, Two macrophages, as boxed in **B** (1 and 2), were filmed for 20 min, and their movement was recorded both as part of the image of the cell (**top**) and as a graphical representation (**bottom**). The movement index is indicated in microns over time in minutes. **D**, Snapshots from intravital imaging of ear vessels after VEGFA (5 μg/mL) treatment. Two individual cells are shown. **E**, Similarly, as in **C**, two macrophages, as boxed in **D** (1 and 2) were filmed for 20 min, and their movement was recorded both as part of the image of the cell (**top**) and as a graphical representation (**bottom**). The movement index is indicated in microns over time in minutes. Note that although both oscillate ≈1 μm, the cell in position 2 is actually moving, as indicated by the color ghosts remaining on the left side of the image. **F**, Quantification of the movement of macrophages recording over time (total of 20 min). Each data point is the average of macrophages in 1 frame (about a hundred cells). Ten frames were evaluated in 3 animals for the no-VEGF condition, and 12 frames were evaluated total within 4 animals in the VEGF condition. Statistics: Welch 2-sample *t* test P=0.0427.

the locations occupied by the cell within a window of time (Figure 5C and 5E, top). In addition, cell motility was graphed every 2 minutes and shown as a single image (Figure 5C and 5E, bottom). Using this approach, the motility and actual migration of macrophages on VEGFA treatment was evident, whereas movement was barely detectable in the absence of VEGFA. To exclude the possibility of any arbitrary bias and to gain a greater perspective on macrophage motility overall, we also evaluated all perivascular macrophages located in a given frame (60–150 cells) in a 20-minute interval. Ten frames were evaluated across several different animals per group (with VEGFA, n=4 or without VEGFA treatment, n=3; Figure 5F). The data clearly demonstrate a strong positive correlation between vascular permeability and macrophage motility.

Macrophage's Binding to ECs Decreases on Induction of Vascular Permeability

To investigate whether different subtypes of macrophages would have different effects on vascular permeability, we first examined their affinity to ECs in vitro. Surprisingly, M1-like macrophages exhibited much less binding to ECs when compared with M2-like macrophages (Figure 6A and 6B).

From intravital imaging analysis (Figure 5A), we were able to capture macrophages detaching from a vessel after administration of VEGFA. However, detachment events were not frequent in the 20-minute intravital imaging time window. Therefore, we resorted to in vitro culture experiments to evaluate macrophage dissociation on permeability induction in a longer time frame. We treated macrophages (M1-like or M2-like) and mouse ECs cocultures with the permeability factor, VEGFA, and observed dissociation of macrophages, particularly M2-like, on treatment (Figure 6C). To confirm this finding in vivo, we treated animals with adenovirus-expressing VEGFA and examined macrophage localization compared with animals injected with control adenoviral particles. We observed a similar detachment effect—not only did macrophages lose association with vessels (Figure 6D; Figure VIA in the online-only Data Supplement), but the total area covered by macrophages relative to vessels was also reduced (Figure VIB in the online-only Data Supplement). Interestingly, the macrophages showed changes in morphology as well (Figure 6D). Quantification of macrophage dissociation from vessels was performed by flow cytometry on peritoneal lavage for F4/80 and Mrc1 double-positive cells after a single injection (1 μg of VEGFA intravenous; or vehicle control). We found that it took ≈60 minutes to notice a significant detachment of macrophages from vessels (Figure 6E).

Phosphorylation of VE-Cadherin Regulates Macrophage-Mediated Permeability

To gain insight into the molecular mechanism underlying the effect of M1-like versus M2-like macrophages on endothelial barrier function, we used in vitro electric cell-substrate impedance sensing to measure the current conduction across a cellular layer. A confluent monolayer of immortalized ECs were plated on an electrode-embedded plate. Macrophages (iBMMs) were then introduced to the culture. When M2-polarized iBMMs were added to the endothelial monolayer, the monolayer maintained resistance; however, the addition of M1-polarized iBMMs reduced the resistance, suggesting an induction of endothelial permeability (Figure 6F and 6G). When permeability factors, like VEGF and thrombin, were added to this system, respectively, only M2-like macrophages were able to rescue the permeability induced by both mediators (Figure 6H). Intriguingly, we noticed that macrophages tend to have more filopodia and bridge adjacent ECs when the permeability factor was added (Figure 6I). In addition, the localization of β-catenin was redistributed from the cell membrane to the cytosol (Figure 6I). This finding led us to speculate that cell adhesion molecules located upstream of the β-catenin pathway might play a role in macrophage-mediated regulation of endothelial permeability. In fact, Western blots showed that ECs cocultured with M2-like macrophages expressed less phosphorylated VE-cadherin when compared with ECs cocultured with M1-like macrophages or cultured alone (Figure 6J and 6K). These findings indicate that M2-like macrophages control the endothelial barrier, at least in part, through regulating VE-cadherin phosphorylation in ECs.

Discussion

Perivascular cells, such as smooth muscle and pericytes, tightly associate with the endothelial wall and provide structural support and contractility to vessels. This well-established function contrasts the poorly understood role of perivascular macrophages. Here, we sought to address the biological relevance of endothelial–macrophage interactions under homeostatic conditions. Stable associations of M2-like macrophages with vessels were identified at high frequency in both mesentery and dermis. Using real-time microscopy, we found that removal of macrophages conveyed a hyperpermeable response to the endothelium on challenge, through a process that required increased macrophage motility and dissociation from the vascular wall. Importantly, reconstitution of M2-like macrophages, but not of M1-like macrophages or dendritic cells, rescued a compromised vascular barrier in macrophage-depleted tissues. To be noted, different subtypes of macrophages affiliate and contribute to the endothelial barrier in different ways. The findings point to a significant role of macrophages in mediating the homeostasis of vascular permeability.

The maintenance of vascular barrier function has been extensively studied, albeit the majority of such studies have focused on either transcellular or intercellular pathways. The contribution of heterotypic cell interactions in vascular barrier has only recently gained credence after a preponderance of evidence that pericytes are essential contributors to barrier integrity, particularly in the brain. The most direct proof came from studies using a variety of platelet-derived growth factor signaling deficient mice that have significantly decreased number of pericytes. Reduction of pericyte coverage in the brain (*Pdgfb*$^{+/-}$, *Pdgfb-F7*) resulted in blood–brain barrier breakdown and accumulation of plasma-derived proteins, ultimately leading to learning and memory deficiencies.[25] Using a slightly different model (*Pdgfb*$^{ret/ret}$ mice), Armulik et al[26] also showed that reduction in pericytes increased permeability and altered the gene expression profile of both ECs and astrocytes. These conclusions were supported by developmental studies that demonstrated a direct correlation between permeability in

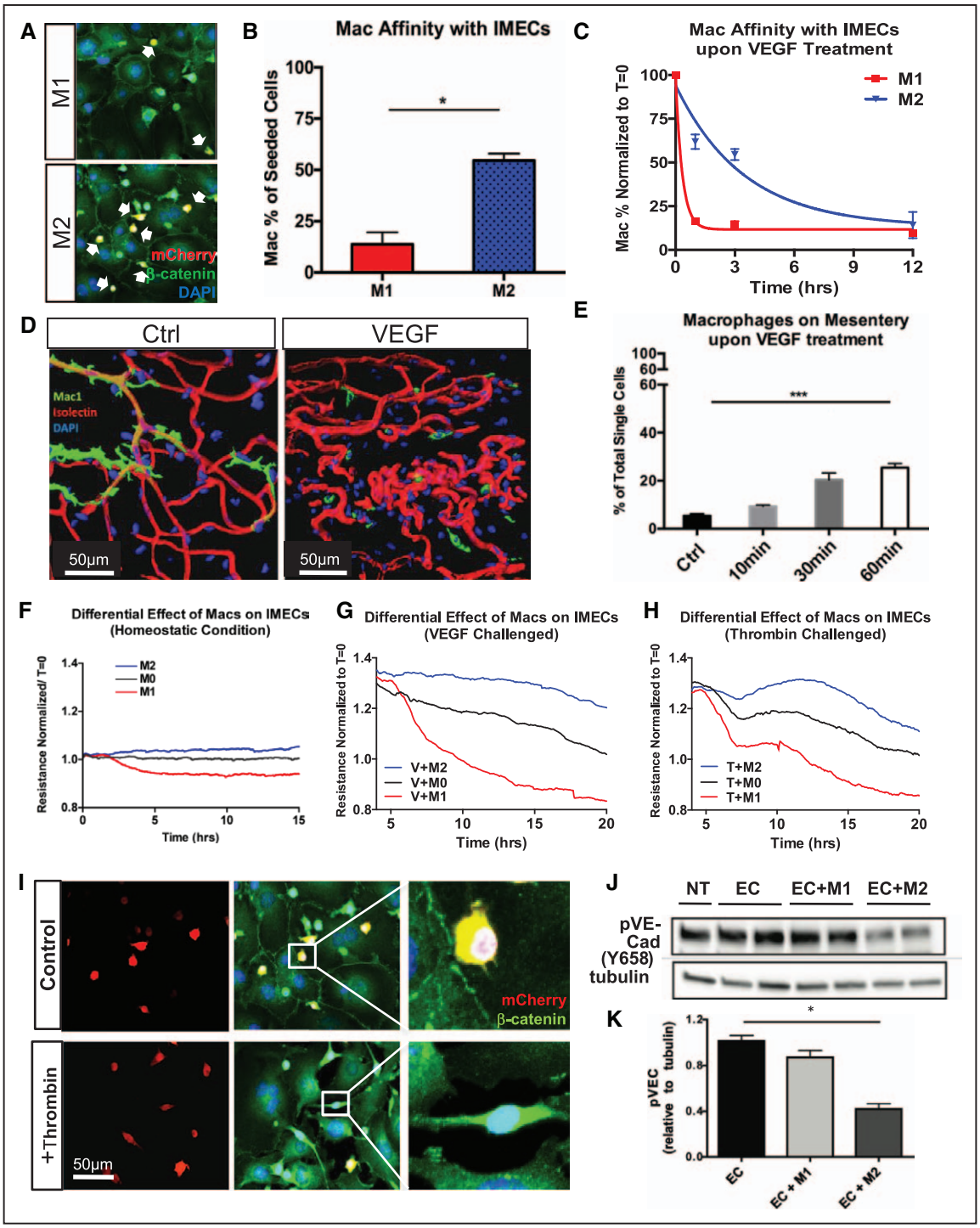

Figure 6. Heterotypic endothelial–macrophage interactions contribute to regulate permeability. **A**, Fluorescent micrographs of macrophages (mCherry labeled) adherent to immortalized endothelial cells (IMECs). **B**, Quantification of the attachment of M1 and M2 macrophages on IMECs after 6 h. n=4. Statistics: Wilcoxon rank-sum test, *P*=0.0286. **C**, Quantification of the adherence of M1 and M2 macrophages on IMECs on VEGFA (Vascular Endothelial Growth Factor A) treatment over time. VEGF, 100 ng/mL. n=3. Statistics: Data were tested as Gaussian. **D**, Representative confocal z-stacks (3-dimensional reconstructed) of mesenteric vessels and macrophages in an adeno-VEGFA–treated animal and control. **E**, Percentage of free macrophages in the mesentery after injection of a single bolus of VEGF (1 μg). Statistics: Data were tested as Gaussian. ***P<0.001 (unpaired Student t test). **F**, **G**, and **H**, Effect of different subtypes of macrophages on endothelial barrier under homeostatic condition (**F**), or after challenge by VEGFA (200 ng/mL; **G**) or Thrombin (10 U/mL; **H**). M0 indicates macrophages without activation; M1, immortal bone marrow macrophages (iBMMs) polarized by lipopolysaccharide (LPS; 50 ng/mL); and M2, iBMMs polarized by interleukin (IL)-4 (10 ng/mL). Data were tested as Gaussian. **I**, Confocal microscopy showing the association of macrophages and IMECs. Macrophages (mCherry-labeled) bridge adjacent endothelial cells after exposure to thrombin. **J**, Expression of phosphorylated VE-cadherin is decreased in endothelial cells (EC) that are cocultured with M2-like macrophages. M1 indicates macrophages polarized by LPS (50 ng/mL); M2, macrophages polarized by IL-4 (10 ng/mL); and NT, nontreated with thrombin. **K**, Quantification of phosphorylated VE-cadherin expression. n=3. Statistics: Wilcoxon rank-sum test, *P*=0.1143 (for EC vs EC+M1), *P*=0.0286 (for EC vs EC+M2).

the blood–brain barrier and pericyte loss, concluding that pericyte number determines the relative leakiness of vessels in the central nervous system during development.[27] Mechanistically, these studies and others have indicated that heterotypic interactions between ECs and pericytes are essential for the development of mature tight junctions between ECs, at least in the brain.[27,28] Our findings indicate that interactions of a subset of macrophages with vessels also contribute to the maintenance of endothelial barrier. Moreover, we have demonstrated both in vitro and in vivo that M2-like macrophages contribute to the protection of endothelial barrier, whereas M1-like macrophages disrupt it. In addition, M1-like and M2-like macrophages tend to have different levels of affiliation with ECs in the absence of pathology. This indicates an interesting distinction between macrophage subtypes, and these differences are consistent with the functionally opposite roles of M1-like and M2-like macrophages in cancer and other pathological conditions. Interestingly, under pathological conditions, tumor-associated macrophages have been shown to promote, rather than to suppress vascular permeability.[29] Real-time imaging of a mouse mammary cancer model revealed synchronized tumor cell intravasation and localized blood vessel permeability with TIE2^{hi} macrophages mediating the permeability via VEGFA destabilization of EC junctions.[30] These findings are in direct discordance with our results. However, we speculate that M2-tumor-associated macrophages might be functionally distinct from the M2-like resident macrophages that we studied under homeostatic conditions. An important consideration could also be the embryonic origin of each subset, as recently bone marrow and yolk sac origins have been attributed to distinct populations of macrophages.[31] A comprehensive transcriptional profile, rather than a handful of markers, would clarify this point. Notwithstanding, information from recent human trials might have already offered important insights.

Clinical trials conducted by Roche using CSF1R monoclonal antibody (RG7155) therapy were successful in depleting tumor-associated macrophages from the tumor tissue.[24,32] Importantly, targeting tumor-associated macrophages via the CSF1/CSF1R axis was efficacious and resulted in improvement of patients. However, several side effects were noted, with facial edema being the most common.[33,34] Because delivery of CSF1R inhibitor was applied via intravenous infusion, edema was likely caused by the systemic depletion of macrophages and in areas away from the tumor (ie, face). These findings support the concept put forward by the present study that perivascular macrophages in the dermis offer stability to vascular networks by enhancing barrier function in sites that are disease free.

In this study, the effects on vascular permeability were more clearly detected on challenge with an agonist, perhaps because our depletion was short lived. We used two common permeability agents, VEGF and bradykinin, and inquired as to the potential role of macrophages in each setting. These molecules change permeability through distinct mechanisms and also vary in the time of induced endothelial response. VEGF targets receptors located on the abluminal side of endothelium, whereas bradykinin works through the luminal side. Because of differences in these two permeability mediators, one could expect a distinct protective response by macrophages. It is interesting, however, that in both cases, permeability was augmented by the depletion of macrophages from the tissue.

Furthermore, we noted that application of permeability mediators promoted movement of macrophages on vessels with progressive detachment. Vessel-associated macrophage movement has only been reported in a handful of cases. Al-Roubaie et al[35] claimed that most macrophages are stationary, which is in line with our observations. Gray et al[36] demonstrated that macrophages in contact with the endothelium migrated faster than the ones in the tissue. Interestingly, we noticed that on long-term exposure to permeability factors, macrophages exhibited higher motility, consistent with the fact that macrophages express receptors for these mediators. This may offer a possible mechanism of how macrophages dynamically regulate permeability. Nonetheless, whether such motility is the cause or the consequence of vascular leakage is still unknown. In fact, the present study did not delve into the mechanism by which macrophages limit vascular permeability. Additional investigations will be necessary to depict the array of heterotypic interactions between endothelial–macrophages and identify cell surface and secreted molecules involved in the regulation of barrier function. Also, questions related to the molecular toolkit that enables some macrophages to navigate and interact with the vasculature are pending. Additional efforts are also needed to clarify the nature of the multiple heterotypic interactions between different subsets of macrophages and the endothelium in vivo. Nonetheless, the findings presented here offer novel information on the functional nature of endothelia–macrophage heterotypic interactions in the context of vascular homeostasis.

Acknowledgments

We thank Dr Carola Ries (Roche Innovation Center Munich) for the supply of the anti-CSF1R antibody, Dr Romain Guiet and Olivier Burri (Bioimaging and Optics Platform at Ecole Polytechnique Fédérale de Lausanne) for their technical support of imaging data analysis, Dr Robert Modlin for providing peripheral blood mononuclear cells, Dr Elisabetta Dejana for providing the antiphospho-VE-cadherin antibody, and Flow Cytometric Facility of the JCCC (University of California Los Angeles) for flow cytometry technical support. We also thank Drs David Elashoff and Daniel Hercz for statistical analysis of the data. H. He, M.A. Swartz, M. De Palma, and M. Luisa Iruela-Arispe designed the research. H. He, E. Güç, W.W. Kilarski, S. Ziyad, and C. Baer performed the intravital imaging, permeability assays, and data analysis. H. He and J.J. Mack performed immunofluorescence staining of tissue samples and confocal imaging analysis. H. He, M.L. Squadrito, C. Baer, A.I. McDonald, and M. Luisa Iruela-Arispe developed immortalized macrophages and performed peritoneal macrophage depletion experiments and permeability assays. C.M. Warren and R.D. Freshman investigated the molecular mechanism of VE-cadherin in macrophage-mediated permeability. H. He, J.J. Mack, and M. Luisa Iruela-Arispe wrote the article.

Sources of Funding

The study was supported by funding from the National Institutes of Health and NHLBI to M. Luisa Iruela-Arispe (HL130290), the California Institute for Regenerative Medicine Award (RB1-01328), and the Swiss National Science Foundation (31003A_143978) to M. De Palma. J.J. Mack was supported by HL069766.

Disclosures

None.

References

1. Davies LC, Jenkins SJ, Allen JE, Taylor PR. Tissue-resident macrophages. *Nat Immunol*. 2013;14:986–995. doi: 10.1038/ni.2705.
2. Mantovani A, Biswas SK, Galdiero MR, Sica A, Locati M. Macrophage plasticity and polarization in tissue repair and remodelling. *J Pathol*. 2013;229:176–185. doi: 10.1002/path.4133.
3. Murray PJ, Wynn TA. Protective and pathogenic functions of macrophage subsets. *Nat Rev Immunol*. 2011;11:723–737. doi: 10.1038/nri3073.
4. Pollard JW. Trophic macrophages in development and disease. *Nat Rev Immunol*. 2009;9:259–270. doi: 10.1038/nri2528.
5. Baer C, Squadrito ML, Iruela-Arispe ML, De Palma M. Reciprocal interactions between endothelial cells and macrophages in angiogenic vascular niches. *Exp Cell Res*. 2013;319:1626–1634. doi: 10.1016/j.yexcr.2013.03.026.
6. De Palma M, Venneri MA, Roca C, Naldini L. Targeting exogenous genes to tumor angiogenesis by transplantation of genetically modified hematopoietic stem cells. *Nat Med*. 2003;9:789–795. doi: 10.1038/nm871.
7. Giraudo E, Inoue M, Hanahan D. An amino-bisphosphonate targets MMP-9-expressing macrophages and angiogenesis to impair cervical carcinogenesis. *J Clin Invest*. 2004;114:623–633. doi: 10.1172/JCI22087.
8. De Palma M, Venneri MA, Galli R, Sergi Sergi L, Politi LS, Sampaolesi M, Naldini L. Tie2 identifies a hematopoietic lineage of proangiogenic monocytes required for tumor vessel formation and a mesenchymal population of pericyte progenitors. *Cancer Cell*. 2005;8:211–226. doi: 10.1016/j.ccr.2005.08.002.
9. Lin EY, Li JF, Gnatovskiy L, Deng Y, Zhu L, Grzesik DA, Qian H, Xue XN, Pollard JW. Macrophages regulate the angiogenic switch in a mouse model of breast cancer. *Cancer Res*. 2006;66:11238–11246. doi: 10.1158/0008-5472.CAN-06-1278.
10. Jetten N, Verbruggen S, Gijbels MJ, Post MJ, De Winther MP, Donners MM. Anti-inflammatory M2, but not pro-inflammatory M1 macrophages promote angiogenesis in vivo. *Angiogenesis*. 2014;17:109–118. doi: 10.1007/s10456-013-9381-6.
11. Fantin A, Vieira JM, Gestri G, Denti L, Schwarz Q, Prykhozhij S, Peri F, Wilson SW, Ruhrberg C. Tissue macrophages act as cellular chaperones for vascular anastomosis downstream of VEGF-mediated endothelial tip cell induction. *Blood*. 2010;116:829–840. doi: 10.1182/blood-2009-12-257832.
12. Outtz HH, Tattersall IW, Kofler NM, Steinbach N, Kitajewski J. Notch1 controls macrophage recruitment and Notch signaling is activated at sites of endothelial cell anastomosis during retinal angiogenesis in mice. *Blood*. 2011;118:3436–3439. doi: 10.1182/blood-2010-12-327015.
13. Das A, Sinha M, Datta S, Abas M, Chaffee S, Sen CK, Roy S. Monocyte and macrophage plasticity in tissue repair and regeneration. *Am J Pathol*. 2015;185:2596–2606. doi: 10.1016/j.ajpath.2015.06.001.
14. Okabe Y, Medzhitov R. Tissue-specific signals control reversible program of localization and functional polarization of macrophages. *Cell*. 2014;157:832–844. doi: 10.1016/j.cell.2014.04.016.
15. Rosas M, Davies LC, Giles PJ, Liao CT, Kharfan B, Stone TC, O'Donnell VB, Fraser DJ, Jones SA, Taylor PR. The transcription factor Gata6 links tissue macrophage phenotype and proliferative renewal. *Science*. 2014;344:645–648. doi: 10.1126/science.1251414.
16. Gosselin D, Link VM, Romanoski CE, Fonseca GJ, Eichenfield DZ, Spann NJ, Stender JD, Chun HB, Garner H, Geissmann F, Glass CK. Environment drives selection and function of enhancers controlling tissue-specific macrophage identities. *Cell*. 2014;159:1327–1340. doi: 10.1016/j.cell.2014.11.023.
17. Lavin Y, Winter D, Blecher-Gonen R, David E, Keren-Shaul H, Merad M, Jung S, Amit I. Tissue-resident macrophage enhancer landscapes are shaped by the local microenvironment. *Cell*. 2014;159:1312–1326. doi: 10.1016/j.cell.2014.11.018.
18. Okabe Y, Medzhitov R. Tissue biology perspective on macrophages. *Nat Immunol*. 2016;17:9–17. doi: 10.1038/ni.3320.
19. He H, Xu J, Warren CM, Duan D, Li X, Wu L, Iruela-Arispe ML. Endothelial cells provide an instructive niche for the differentiation and functional polarization of M2-like macrophages. *Blood*. 2012;120:3152–3162. doi: 10.1182/blood-2012-04-422758.
20. Hanna RN, Cekic C, Sag D, et al. Patrolling monocytes control tumor metastasis to the lung. *Science*. 2015;350:985–990. doi: 10.1126/science.aac9407.
21. Armulik A, Genové G, Betsholtz C. Pericytes: developmental, physiological, and pathological perspectives, problems, and promises. *Dev Cell*. 2011;21:193–215. doi: 10.1016/j.devcel.2011.07.001.
22. Brown LF, Guidi AJ, Tognazzi K, Dvorak HF. Vascular permeability factor/vascular endothelial growth factor and vascular stroma formation in neoplasia. Insights from in situ hybridization studies. *J Histochem Cytochem*. 1998;46:569–575.
23. Svensjö E, Cyrino F, Michoud E, Ruggiero D, Bouskela E, Wiernsperger N. Vascular permeability increase as induced by histamine or bradykinin is enhanced by advanced glycation endproducts (AGEs). *J Diabetes Complications*. 1999;13:187–190.
24. Ries CH, Cannarile MA, Hoves S, et al. Targeting tumor-associated macrophages with anti-CSF-1R antibody reveals a strategy for cancer therapy. *Cancer Cell*. 2014;25:846–859. doi: 10.1016/j.ccr.2014.05.016.
25. Bell RD, Winkler EA, Sagare AP, Singh I, LaRue B, Deane R, Zlokovic BV. Pericytes control key neurovascular functions and neuronal phenotype in the adult brain and during brain aging. *Neuron*. 2010;68:409–427. doi: 10.1016/j.neuron.2010.09.043.
26. Armulik A, Genové G, Mäe M, Nisancioglu MH, Wallgard E, Niaudet C, He L, Norlin J, Lindblom P, Strittmatter K, Johansson BR, Betsholtz C. Pericytes regulate the blood-brain barrier. *Nature*. 2010;468:557–561. doi: 10.1038/nature09522.
27. Daneman R, Zhou L, Kebede AA, Barres BA. Pericytes are required for blood-brain barrier integrity during embryogenesis. *Nature*. 2010;468:562–566. doi: 10.1038/nature09513.
28. Kim JH, Kim JH, Yu YS, Kim DH, Kim KW. Recruitment of pericytes and astrocytes is closely related to the formation of tight junction in developing retinal vessels. *J Neurosci Res*. 2009;87:653–659. doi: 10.1002/jnr.21884.
29. Moughon DL, He H, Schokrpur S, Jiang ZK, Yaqoob M, David J, Lin C, Iruela-Arispe ML, Dorigo O, Wu L. Macrophage blockade using CSF1R inhibitors reverses the vascular leakage underlying malignant ascites in late-stage epithelial ovarian cancer. *Cancer Res*. 2015;75:4742–4752. doi: 10.1158/0008-5472.CAN-14-3373.
30. Harney AS, Arwert EN, Entenberg D, Wang Y, Guo P, Qian BZ, Oktay MH, Pollard JW, Jones JG, Condeelis JS. Real-time imaging reveals local, transient vascular permeability, and tumor cell intravasation stimulated by TIE2hi macrophage-derived VEGFA. *Cancer Discov*. 2015;5:932–943. doi: 10.1158/2159-8290.CD-15-0012.
31. Gomez Perdiguero E, Klapproth K, Schulz C, Busch K, Azzoni E, Crozet L, Garner H, Trouillet C, de Bruijn MF, Geissmann F, Rodewald HR. Tissue-resident macrophages originate from yolk-sac-derived erythro-myeloid progenitors. *Nature*. 2015;518:547–551. doi: 10.1038/nature13989.
32. Brahmi M, Vinceneux A, Cassier PA. Current systemic treatment options for tenosynovial giant cell tumor/pigmented villonodular synovitis: targeting the CSF1/CSF1R axis. *Curr Treat Options Oncol*. 2016;17:10. doi: 10.1007/s11864-015-0385-x.
33. Tap WD, Wainberg ZA, Anthony SP, et al. Structure-Guided Blockade of CSF1R Kinase in Tenosynovial Giant-Cell Tumor. *N Engl J Med*. 2015;373:428–437. doi: 10.1056/NEJMoa1411366.
34. Cassier PA, Italiano A, Gomez-Roca CA, et al. CSF1R inhibition with emactuzumab in locally advanced diffuse-type tenosynovial giant cell tumours of the soft tissue: a dose-escalation and dose-expansion phase 1 study. *Lancet Oncol*. 2015;16:949–956. doi: 10.1016/S1470-2045(15)00132-1.
35. Al-Roubaie S, Hughes JH, Filla MB, Lansford R, Lehoux S, Jones EA. Time-lapse microscopy of macrophages during embryonic vascular development. *Dev Dyn*. 2012;241:1423–1431. doi: 10.1002/dvdy.23835.
36. Gray C, Loynes CA, Whyte MK, Crossman DC, Renshaw SA, Chico TJ. Simultaneous intravital imaging of macrophage and neutrophil behaviour during inflammation using a novel transgenic zebrafish. *Thromb Haemost*. 2011;105:811–819. doi: 10.1160/TH10-08-0525.

Highlights

- A subset of M2-like macrophages associate with small-diameter vessels at high frequency.
- Under homeostatic conditions, perivascular macrophages enhance endothelial barrier function and restrain hyperpermeable responses.
- Macrophage-mediated suppression of permeability occurs, at least in part, through regulation of VE-cadherin phosphorylation.

Arteriosclerosis, Thrombosis, and Vascular Biology

JOURNAL OF THE AMERICAN HEART ASSOCIATION

Perivascular Macrophages Limit Permeability

Huanhuan He, Julia J. Mack, Esra Güç, Carmen M. Warren, Mario Leonardo Squadrito, Witold W. Kilarski, Caroline Baer, Ryan D. Freshman, Austin I. McDonald, Safiyyah Ziyad, Melody A. Swartz, Michele De Palma and M. Luisa Iruela-Arispe

Arterioscler Thromb Vasc Biol. 2016;36:2203-2212; originally published online September 15, 2016;
doi: 10.1161/ATVBAHA.116.307592
Arteriosclerosis, Thrombosis, and Vascular Biology is published by the American Heart Association, 7272 Greenville Avenue, Dallas, TX 75231

Print ISSN: 1079-5642. Online ISSN: 1524-4636

Mice

Wild type (C57BL/6J) mice, nude mice and B6C3Fe-a/a-Csf1op/J mice were obtained from the Jackson Laboratory (Bar Harbor, ME). Animal protocols were reviewed and approved by the UCLA Institutional Animal Care and Use Committee.

Cell culture

Bone marrow cells were isolated from wild type animals by flushing the bone marrow, dissociating the cells with a mild trypsin solution and followed by lysis of red blood cells for 5min using the ACK lysing buffer (Thermo Fisher). Cells were then suspended in macrophage medium (alpha-MEM (Gibco) with 10% fetal bovine serum (Omega Scientific Inc.) and M-CSF (PeproTech) and plated for seven days with medium change on day three. Bone marrow macrophages were then used for experiments. For dendritic cell isolation, bone marrow was flushed from the tibia and femur and cells were cultured in RPMI 1640 medium supplemented with 10% fetal bovine serum (Gibco), 50uM beta-mercaptoethanol (Sigma-Aldrich) and 20 ng/ml GM-CSF. Medium was changed every 2-3 days and cells were cultured for 6-7 days. Immortal bone marrow macrophages (iBMMs) (**Suppl. Fig. 4A-C**) were generated using an immortalizing lentiviral vector and confirmed to express macrophage-specific markers[1]. Immortalized mouse ECs (IMECs) were cultured as previously described[2].

Mesentery preparation, immunostaining and confocal microscopy

Intestine and mesentery was dissociated from animals and fixed with 2% paraformaldehyde (PFA) for six hours. Samples were washed thoroughly with PBS and the mesentery was then cut into 0.2-0.5 cm fragments and stored in 1X PBS before staining. Immunofluorescence was performed using standard procedures. Briefly, segments from the mesentery in between larger vessels and poor in adipocytes (mesenteric windows) were dissected and permeabilized in 0.3% Triton-X (Sigma) in 1X PBS for five minutes and then blocked in 1X PBST (0.05% Tween20 in 1X PBS) with 3% normal donkey serum for 20 minutes. Primary antibodies were applied for 60 minutes, including Isolectin GS-IB4 Alexa Fluor® 594 Conjugate (Life Technologies), anti-mouse F4/80 (Serotech), biotin-CD206 (Biolegend), anti-mouse Mrc1 (Santa Cruz), anti-mouse CD11b (BD Biosciences) and anti-mouse NG2 (Millipore). DAPI (Invitrogen) was used to stain nuclei. A confocal microscope (LSM710, Carl Zeiss) equipped with Zeiss EC Plan-Neofluar 40X/1.3 oil objective was used for image acquisition at room temperature.

For 3D reconstructions, confocal z-stacks were imported into Imaris software version 7.7.1 (Bitplane). Multi-color 3D visualization was achieved by iso-surface rendering of each channel.

Flow cytometry

Mesenteric cells were dissociated using collagenase (Gibco) and incubated at 37°C for 45 minutes. The digested tissue solution was passed through 40 µm filter (BD Biosciences) and spun down at 250xg for five minutes. Single cells were then re-suspended in FACS buffer (1X HBSS (CellGro) with 2% FBS (Omega Scientific Inc.) and 10mM HEPES (Gibco)). Antibodies used were APC-eFluor780-F4/80 (eBioscience), FITC-Mac1 (eBioscience), biotin-CD206 (Biolegend) and mouse anti-

NG2 (Millipore). Secondary antibodies used were 488-Streptoavidin (Invitrogen) and 488-anti mouse (Invitrogen). For endogenous Fc blocking, cell suspensions were preincubated with Mouse BD Fc Block™ (BD Biosciences) purified anti-mouse CD16/CD32 mAb 2.4G2 (≤ 1 µg/million cells in 100 µl, i.e., 1:50 with 0.5mg/ml) at 4˚C for 10 minutes. For FACS experiment the following controls were included: primary antibody control, isotype controls, compensations controls for each fluorochrome, cell viability controls (PI staining), and specificity controls. In specificity controls, a ten-fold excess unlabeled primary antibody was used together with the standard amount of the primary antibody.

LSRII Analytic Flow Cytometer (BD Biosciences) was used for acquisition. Data was analyzed with FlowJo (Tree Star Inc.).

Vessel permeability assay on macrophage-depleted skin

8-12 weeks old nude male mice were used in all experiments. Two days prior to imaging, dorsal skin of mouse ears received two injections, 5µl each of either clodronate liposomes (5 mg/ml; Clodronate Liposomes) or PBS (control) liposomes (Clodronate Liposomes). Surgical procedures and live imaging were performed using a fluorescence stereomicroscope with a motorized stage (M250 FA, Leica Microsystems CMS GmbH) equipped with a 1x lens (linear system magnification from 7.5x to 160x) or 2x lens (linear system magnification from 15.6x to 320x), with a resolution range between 7.89 µm (at 15.6x magnification) and 0.95 µm (at 320x magnification) respectively. Images were collected using a DFC 350 FX camera controlled by LAS AF software (Leica). Animal temperature was monitored and controlled throughout the experiment with the DC Temperature Control System (FHC Inc.).

Mice were anesthetized with ketamine/Dorbene (75mg/kg/1mg/kg) and dorsal ear skin was surgically exposed as described[3,4]. Briefly, the ventral skin of the ear was cut along the antihelix of the mouse pinna, followed by separation of cartilage and muscle using the blunt edge of a scalpel. Two additional 1 mm cuts were made at the edge of the ear to prime the separation of the ventral and dorsal parts. The ventral skin and cartilage were then gently pulled apart with curved forceps to separate the ventral and dorsal skin, exposing the dermis at the posterior and midsections of the ear and the hypodermis at the anterior side. The side corners of the exposed dorsal ear dermis were glued to the supporting glass slide and ears were stained for 15 minutes with biotinylated rabbit anti-collagen type IV (Abcam) and CD206-APC (Biolegend) antibodies, washed briefly with Ringer's buffer (102 mM NaCl, 5 mM KCl, 2 mM CaCl2, 28 mM sodium lactate) and incubated for additional 15 minutes with streptavidin-Pacific Blue (Invitrogen). Primary antibodies and streptavidin-Pacific Blue were mixed in Ringer's buffer supplemented with 125 IU/ml (2.5 mg/ml) aprotinin and kept at 4°C before being pipetted onto the exposed ear dermis. Then, 200 µl of 10 mg/ml 155 kDa TRITC-Dextran (Invitrogen) was injected intravenously and 6 to 8 fields in the area where liposomes had been injected were imaged every 1 minute for up to 30 minutes. Subsequently, blood vessel leakage was stimulated either with topical application of 40 µl of 5 µg/ml VEGF-165 (Peprotech) in PBS or intravenous injection of 50 µl of 4 mg/ml of bradykinin in PBS and the same fields were imaged for an additional 30 minutes.

Quantification of the leakage was analyzed using Leica LAS AF software. The experiments were repeated with six mice per experimental group.

Vessel permeability after peritoneal macrophage depletion and reconstitution

Clodronate and control liposomes (described in 'Vessel permeability assay on macrophage-depleted skin') were injected via intraperitoneal injection (i.p.) with 200μl/mouse on day 1. On day 3, liposomes were injected again following the same method. Bone marrow derived macrophages (10^6 cells in 100μl PBS) were delivered via intravenous injection (i.v.). Three to five mice were used for each experimental group. Two days later, 100μl FITC-ovalbumin or TRITC-dextran (Invitrogen) were injected i.v. in each mouse. After specific time intervals, animals were euthanized and 1ml of PBS was injected i.p. to recover the peritoneal macrophages and liquid in the peritoneal cavity. The solution was then spun down, from which the supernatant was taken for fluorescence intensity quantification and the cell pellet was re-suspended in FACS buffer for flow cytometric analysis (see 'Flow cytometry' section). The fluorescence intensity was read by SAFIRE II (V4.62n). In the case of antibody depletion, 30mg/kg anti-CSF-1R antibody (clone 2G2)[5] was applied i.p. weekly for four consecutive weeks. Animals were then euthanized for permeability analysis as described above or used for reconstitution experiments. For these experiments, clearance of anti-CSF1-R antibody from the circulation was first evaluated by ELISA. In general 7-10 days were necessary after the last injection, at which time no increase in the number of endogenous macrophages was detected.

For reconstitution, iBMMs were polarized into different subtypes as previously described[2] and characterized for M1 and M2 markers as shown in Suppl. Figure 5. Cells were then delivered by i.v. injection into animals (10^6 per animal). After three days, animals were subjected to permeability assessment.

For macrophage extravasation assay, mCherry labeled iBMMs (10^6 per animal) were injected i.v.. After 16 hours, peritoneal macrophages were recovered as previously described. The cells were then stained with FITC-Mac1 (eBioscience) antibody for flow cytometric analysis (see 'Flow cytometry' section).

In vivo macrophage motility analysis

Time-stacks were acquired as described under 'Vessel permeability assays on macrophage-depleted skin'. This allowed the recording of blood vessels and cells in two distinct fluorescent channels (the two channels will be referred to as "vessel-channel" and "cell-channel"). An automatic registration of each time-stack was performed using the ImageJ plugin "StackReg" to correct for drift due to animal movement during the acquisition[6]. The image was cropped in order to avoid "edge effects" (black area) due to registration. Two different analysis methods were applied, "global" and "frame by frame."

For the "global" analysis, projections of time-stacks were made to identify the vessel vicinity and measure the cell movement in this area. The vessel boundaries were marked by performing a projection calculating the sum of the time-stack ("Sum-projection"). A threshold was then applied by using an automatic algorithm to create a binary mask ("AutoTh"). Briefly, (1) apply "Kittler and Illingworth's Minimum Error

thresholding method" (1986; Fiji, "MinError" auto threshold) on the entire image; (2) obtain the corresponding "Area"; (3) apply "MinError" to the image restricted to the previously detected "Area"; (4) determine the "Area_t+1"; (5) calculate the difference (Area_t – Area_t+1). This recursive processing continues until the difference in "Area" is below a specific value (here, 20%). Then, the last threshold image is saved, "AutoTh."

Alternatively, in cases of a weak signal to noise ratio, the contours of the vessel were drawn manually. The mask was then enlarged by 40 pixels ("Enlarge") and the area between the original and the enlarged mask was created using the XOR operation ("Xor(AutoTh, Enlarge)"). To measure the cell movement, an average "AVG" and a standard deviation "STD" projection of the cell-channel were created. The "STD" displays pixels changing over time and at first approximation this can be linked to the movement of cells. For comparison of stacks with different absolute intensities, the coefficient of variation "CV" can be calculated by dividing the "STD" projection by the "AVG" projection ("STD/AVG(cells)"). The multiplication of the "CV" with the mask defining the area around the vessel gives a measure of mobile cells.

For the "frame by frame" analysis, a threshold was applied to each frame using "Tsai's method" (1985; Fiji, "Moments" auto threshold). Next, for each frame, XOR images were created ("XOR of Frame t and t+1") and the area was measured ("Area (XOR of Frame t and t+1)"). The "Area (XOR of Frame t and t+1)" can then be normalized by the average of the areas of each frame ("Average (Area (Frame t), Area (Frame t+1))"). This displays the pixels changing between two consecutives frames.

Macrophage binding assays

Different subtypes of mCherry-iBMMs (50,000 per well in 6-well plate) were seeded onto a confluent layer of IMECs. After six hours, wells were washed and then cells trypsinized, then re-suspended in FACS buffer (see 'Flow cytometry') and the percentage of mCherry cells was determined. This percentage was then divided by the original percentage of mCherry cells/IMECs.

For detachment assay, VEGF (100 ng/ml) or LPS (50 ng/ml) was introduced into the co-culture of mCherry-iBMMs/IMECs for the time indicated. The percentage of mCherry positive cells was obtained through flow cytometric analysis and normalized to t=0 before treatment.

Macrophage and vessel co-localization analysis in the presence of permeability mediators

Evaluation of the effect of permeability mediators on macrophages binding to capillaries was assessed using two approaches:

(1) Adenovirus-mediated approach. Adenoviral (Ad)-mediated gene transfer into liver cells was accomplished by single bolus injection of 10^{11} Ad particles (corresponding to $5X10^{9}$ PFU as determined on 293 cells) in 200 ul of PBS by tail vein injection. An adenvirus without VEGF (empty vector) was used as control. Prior to injection, the virus preparations were tested to confirmed to be free of endotoxin contamination. Animals were injected with adenovirus expressing VEGF-A or empty adenoviral particles (controls) 16 hours prior to experiments to allow for a robust increase in circulating levels of VEGF, but sufficiently short to prevent other events associated with this robust

VEGF increase. The induced levels of VEGF ranged between 20ng to 150ng/ml. This increase was in contrast to control mice with 12-50pg/ml VEGF levels. All experimental procedures were conducted in accordance with institutional guidelines and following approved protocols.

(2) Bolus injection of protein – For these experiments, we simply injected 1ug of VEGF protein (Peproteck) into 200ul of PBS and waited 6 hours for evaluation.

Mesentery sections were fixed and vessels imaged as described in 'Mesentery preparation, immunostaining and confocal microscopy.' Confocal z-stack images from each group were converted into images using maximum intensity projection. The images were then analyzed for co-localization of the green and red channels using Zen software (Carl Zeiss). Background was corrected in Auto mode. Overlap (Pearson's coefficient) value was used for quantification of co-localization.

Macrophage and IMEC co-culture

IMECs were grown to confluent layer before iBMMs (10^5 per 35mm dish) were added to the culture. Co-cultures were incubated at 37°C overnight. The next day, thrombin (15 U/ml) was added to the co-culture. One hour later, cells were fixed with 1% PFA, permeabilized with 0.01% Triton-X and subject to immunostaining. Primary antibody applied was anti-β-catenin (Sigma). For image acquisition, confocal microscope (LSM710, Carl Zeiss) was used at room temperature.

***In vitro* permeability assay**

Electric cell substrate impedance sensing (ECIS) was performed to measure endothelial barrier function. ECIS array (8W10E+, Applied Biophysics) was calibrated before IMECs were added. The cells were grown at 33°C until confluent. The impedance of the cell culture was then monitored at 37°C. Macrophages (20,000 cells) were added to each well of an ECIS array. For VEGF or thrombin treatment, IMECs were serum starved for six hours before treatment with VEGF (150 ng/ml) or thrombin (30 U/ml). The monolayer was measured for 15-20 minutes and data acquired and analyzed using ECIS software (Applied Biophysics). For the experiments shown in Supplemental Figure IV A, ECIS was also performed using human aortic endothelial cells.

Western blot for VE-cadherin

Human peripheral blood mononucleated cells (PBMCs, provided by Dr. Robert Modlin) were plated in RPMI with 1% FBS for 2 hours at 37°C. Non-adherent cells were washed off and adherent monocytes were cultured in RPMI with 10% FBS and 100ng M-CSF for six days to differentiate into M0 macrophages, then for two days with 50ng/ml IFNg and 10ng/ml LPS to further differentiate into M1-like macrophages, or 20ng/ml IL-4 to differentiate into M2-like macrophages. M1-like or M2-like macrophages (10^5 cells) were seeded on top of a confluent monolayer of human umbilical vein endothelial cells (HUVECs; $2x10^5$ cells) and co-cultured for 24 hours. Co-cultures were then serum starved for six hours and then challenged with 5U/ml thrombin for 15 minutes at 37°C. Co-cultures were washed with PBS then lysed in modified RIPA (mRIPA) buffer (50 mM Tris, pH 7.4, 150 mM NaCl, 1% NP-40, 0.25% sodium deoxycolate, 1 mM EDTA, 1 mM Na_3VO_4, 10 mM β-glycerophosphate, and protease inhibitor cocktail (Roche)). Lysates were agitated at 4°C for 30 minutes and then centrifuged for 10 minutes at 4°C to

remove debris. Proteins were separated by SDS-PAGE gradient (4-20%) gel and immunoblot analysis was performed with antibodies against γ-tubulin (Abcam) and phospho-VE-cadherin Y658 (provided by Dr. Elisabetta Dejana).

Statistics

Statistical analyses were performed in most experiments with the exceptions of qualitative imaging analysis. Drs. Danield Hercz and Dr. David Elashoff (biostatistics core at UCLA) provided oversight and re-evaluated all of the statistics. For every dataset it was first determined whether parametric or non-parametric analysis was appropriate and the use of either t-test or Mann Whitney to assess significance. In some cases one was chose over the other and the selection was clearly noted in the Figure Legends. For figures 2E and 2F there was the option to analyze the data using a "mixed model" approach which would yield a single result (and p-value) comparing the two curves, instead of pairwise comparisons. Both clearly yield significant results. Mixed modeling is typically a more powerful, however, the difference between the curves is quite strong and keeping the pairwise nature of the analysis was selected to be more consistent with the other figures.

References

1. Squadrito ML, Baer C, Burdet F, Maderna C, Gilfillan GD, Lyle R, Ibberson M, De Palma M. Endogenous RNAs modulate MicroRNA sorting to exosomes and transfer to acceptor cells. *Cell Rep*. 2014;8(5):1432-1446.
2. He H, Xu J, Warren CM, *et al*. Endothelial cells provide an instructive niche for the differentiation and functional polarization of M2-like macrophages. *Blood*. 2012;120(15):3152-3162.
3. Kilarski WW, Güç E, Teo JC, Oliver SR, Lund AW, Swartz MA. Intravital immunofluorescence for visualizing the microcirculatory and immune microenvironments in the mouse ear dermis. *PLoS ONE*. 2013;8(2):e57135.
4. Guc E, Fankhauser M, Lund AW, Swartz MA, Kilarski WW. Long-term intravital immunofluorescence imaging of tissue matrix components with epifluorescence and two-photon microscopy. *JoVE* 2014;86:e51388.
5. Ries CH, Cannarile MA, Hoves S, *et a*l. Targeting tumor-associated macrophages with anti-CSF-1R antibody reveals a strategy for cancer therapy. *Cancer Cell*. 2014;25(6):846-859.
6. Thévenaz P, Ruttimann UE, Unser M. A pyramid approach to subpixel registration based on intensity. *IEEE Trans Image Process.* 1998;7(1):27-41.

Suppl. Fig.I Macrophages associate with the endothelium in the lumen and in the extravascular space.

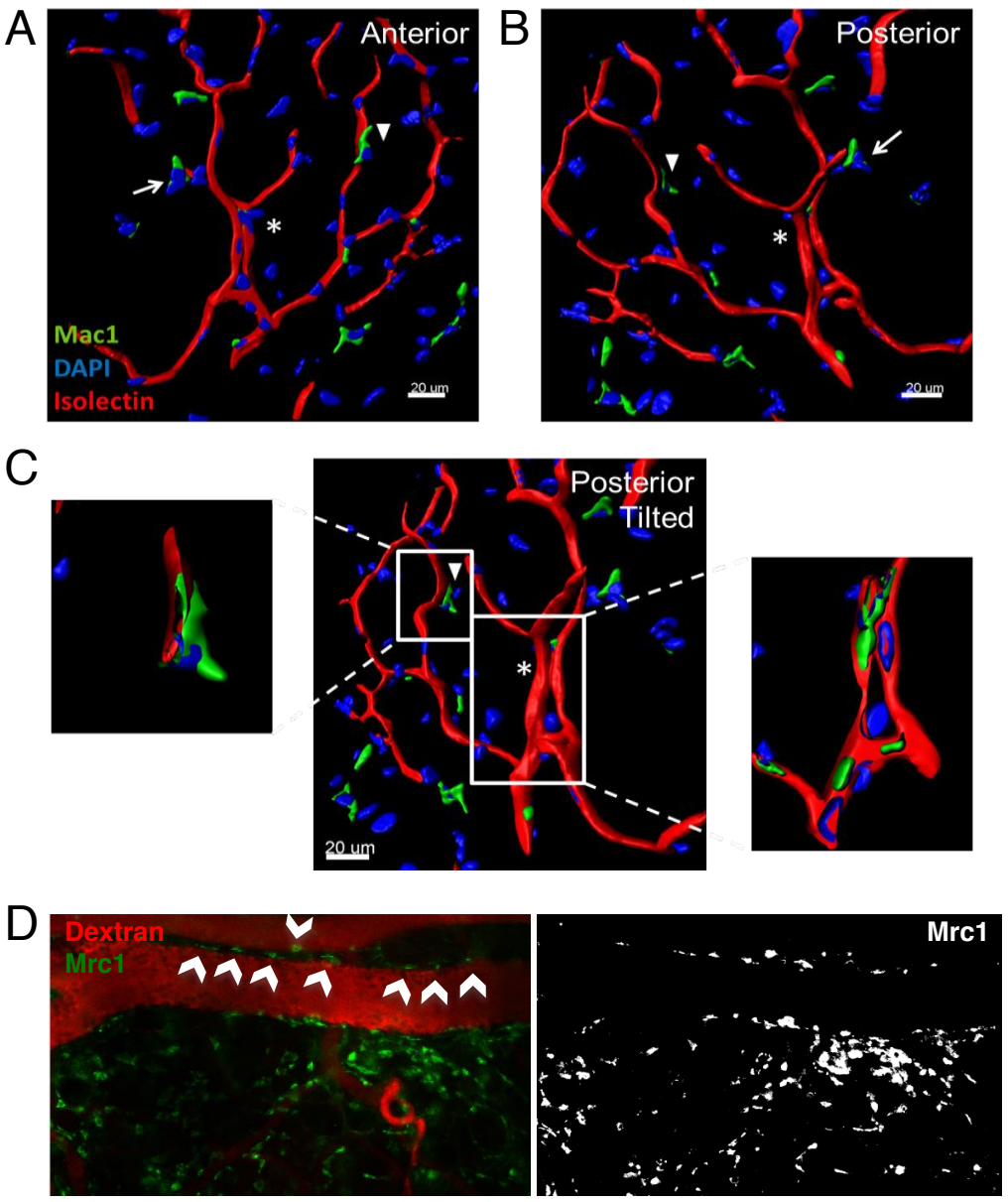

(A-C) Imaging of mesenteric vessels reveals association of macrophages with blood vessels using 3D reconstruction (magnified in boxes) of confocal z-stacks. Images are representative of n=12 mice analyzed. A) Anterior and B) posterior views of the vessel network show macrophages in direct contact with vessel (arrows) and inside vessel wall (asterisk). C) Tilted posterior view and magnified sliced sections (boxes) confirm macrophages in contact with the vessel wall- both inside and outside. Mac1 (CD11b) was used to identify macrophages (green). Isolectin was used to identify vessels (red). DAPI labeled nuclei. D) Intravital imaging of the skin using TRITC-Dextran to label blood vessels and Mrc1 to label macrophages *in vivo (*green*)*. White arrowheads highlight series of Mrc1^{+} cells lining the blood vessel wall. Single channel image for Mrc1 staining is displayed on right.

Suppl. Fig.II Majority of resident macrophages are M2-like.

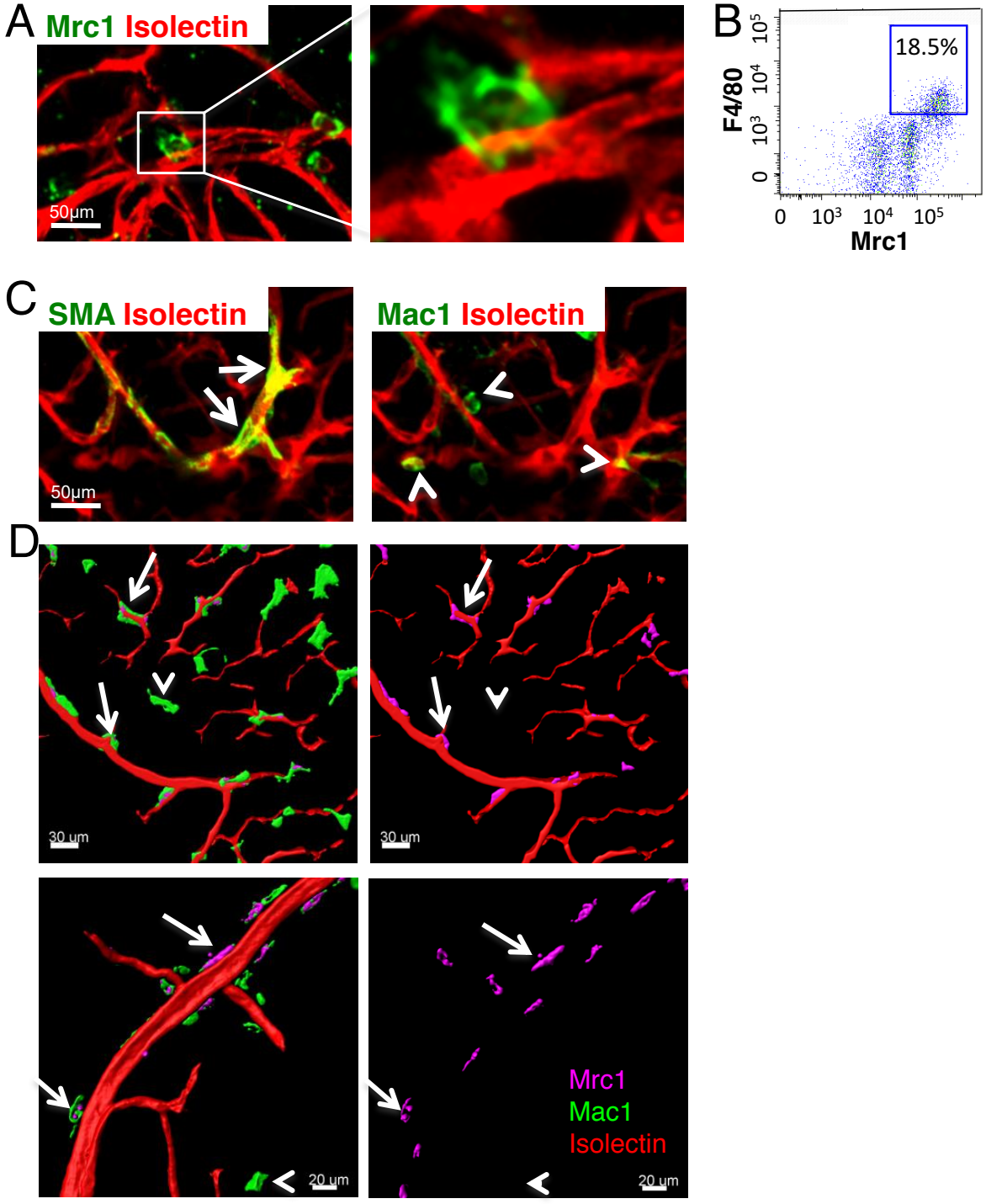

A) Maximum intensity projection of confocal z-stack (magnified on right) of M2-like macrophages (MRC1⁺) in contact with vessels (labeled by Isolectin). B) Quantification of M2-like macrophages on mesentery. Note that the majority of F4/80⁺ cells (19.2%, shown in **Fig. 1C**) are MRC1⁺. C) Localization of SMA⁺ (arrow) and MRC1⁺ (arrowhead) cells on mesentery vessels using maximum intensity projection of confocal z-stacks. D) Evaluation of Mac1(CD11b) and CD206 in perivascular macrophages. Note that macrophages juxtaposed to blood vessels are either Mrc1 (CD206) or double positive for Mrc1 and Mac1 low (arrows). In contrast macrophages that are only Mac1 positive were most frequently not associated with vessels (arrowheads).

Suppl. Fig.III Depletion of resident macrophages enhances vascular permeability.

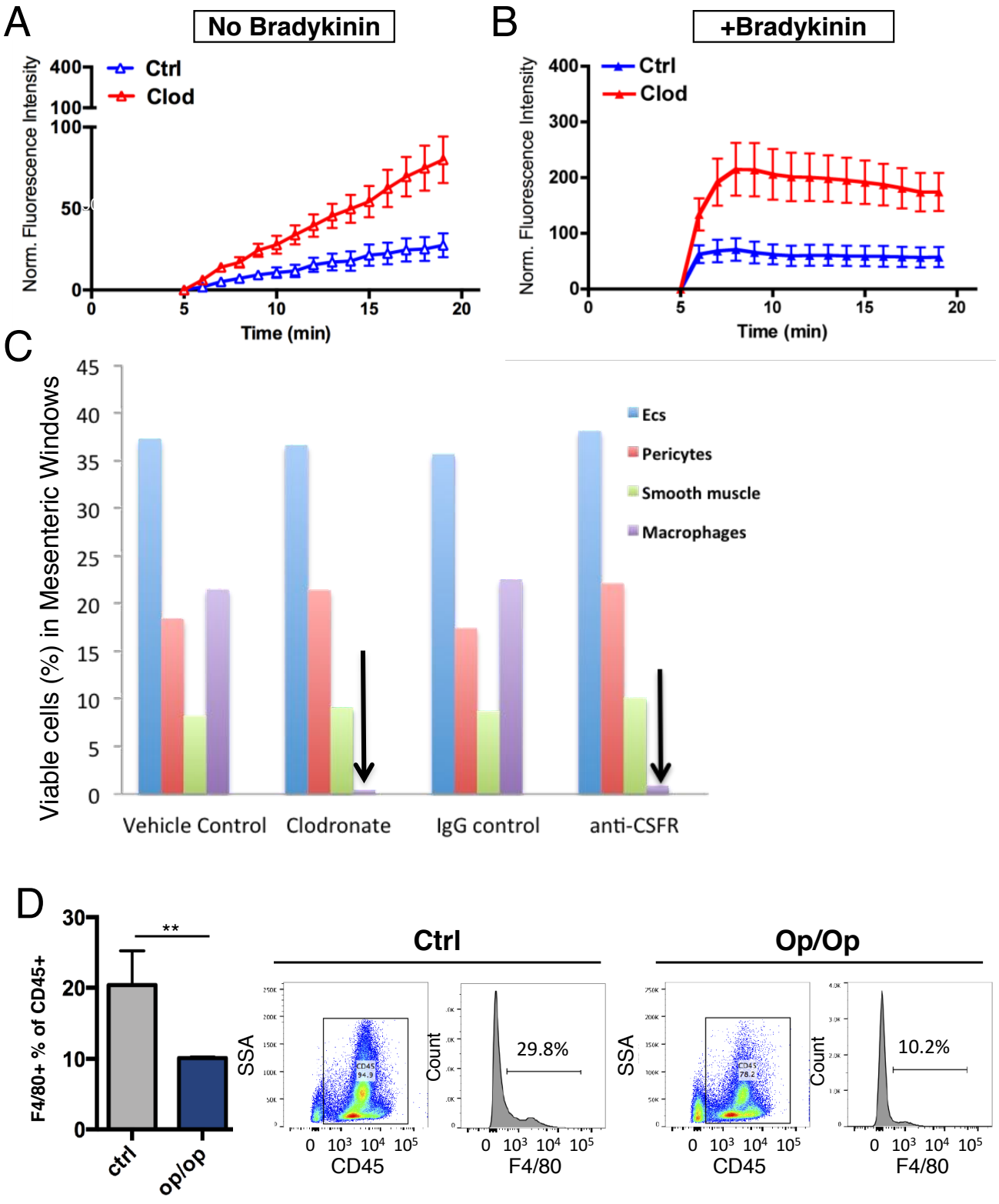

A,B) Quantification of TRITC-Dextran intensity on the ear with (B) or without (A) bradykinin in 20 minutes time course. n=3 for each group. Mixed model analysis was performed and samples were statistically different after 10 min in A and after 6min in B. C) Assessment of viability in different cell populations after treatment with Clodronate (2w) and anti-CSFR (3w). Endothelial cells were identified by CD31 and Cdh5 expression; pericytes were identified by NG2; smooth muscle cells by calponin

Suppl. Fig.IV In the absence of macrophages, anti-CSFR1 does not affect endothelial barrier in vitro or endothelial inflammatory response.

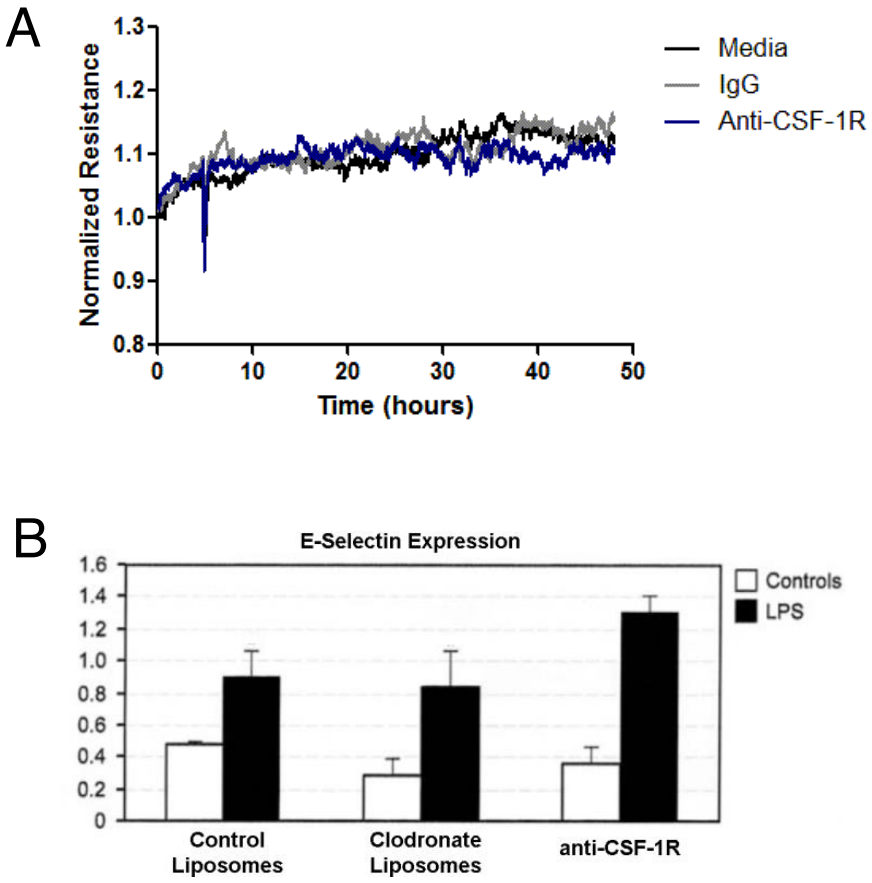

A) Evaluation of IgG (control) and anti-CSF1R antibody on endothelial permeability. Transendothelial resistance was assessed continuously over 50hrs. Shown is a representative experiment from 4 independent evaluations. B) Quantification of E-selectin expression after 8h exposure to control liposomes, clodronate liposomes and anti-CSF1R in the presence or absence of LPS (1ng/ml). n= 3 per experimental treatment.

Suppl. Fig.V Characterization of iBMM (immortal bone marrow macrophages).

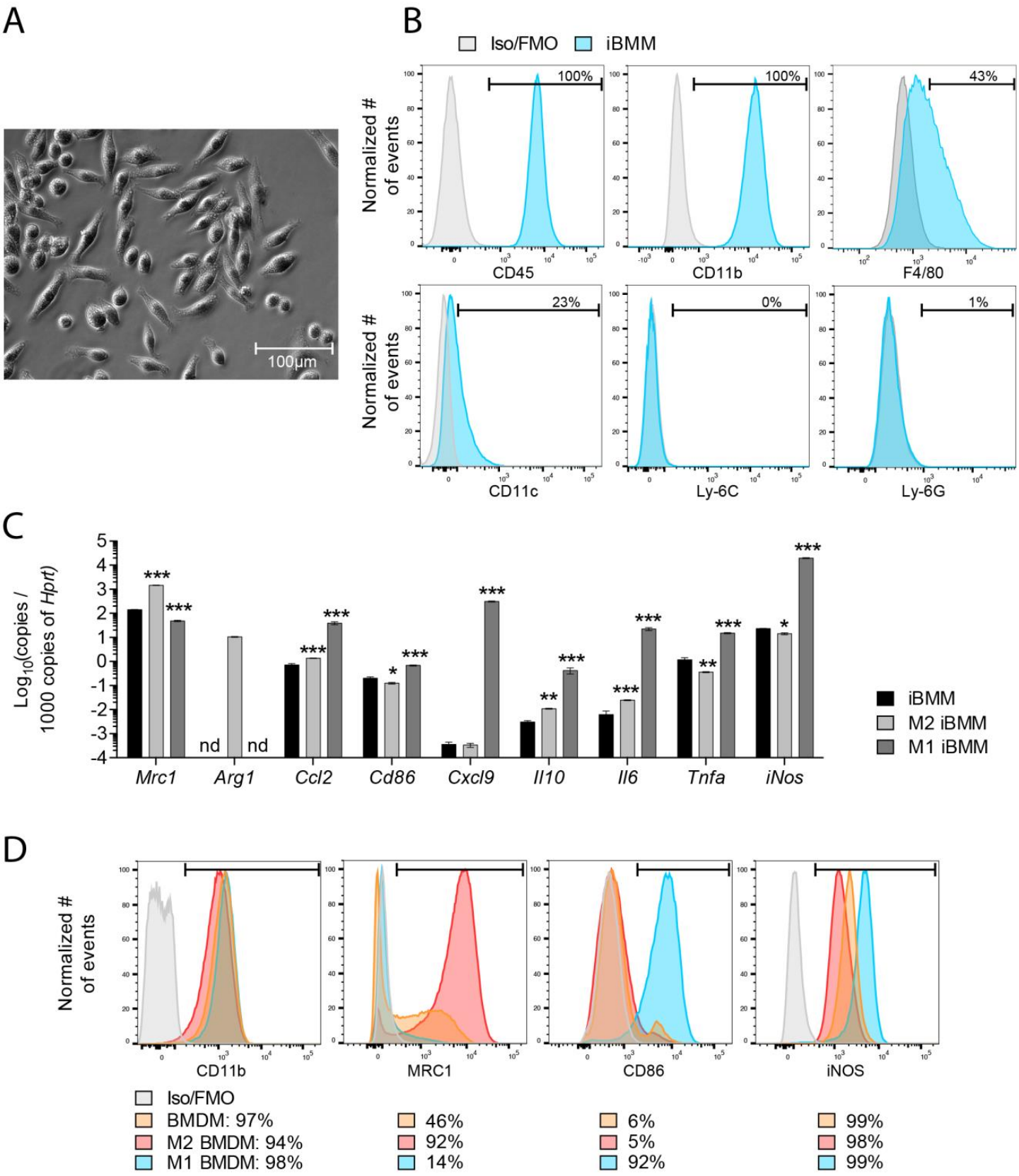

A) Micrograph of iBMMs in culture. B) Characterization of iBMMs by surface markers expression using flow cytometry. Note that most iBMMs express high level of CD11b (or Mac1), F4/80, but not Gr1. C) mRNA expression of indicated markers by polarized iBMMs. *Arg1* and *Mrc1* (M2-like macrophage markers) were up regulated in iBMMs when polarized by IL-4 and *Ccl2, Cd86, Cxcl9, Il10, Il6, Tnfa and iNos* (M1-like macrophage marker) expression was increased when exposed to LPS + IFNg. Normalized to *Hprt*, n=3, ***, p<0.001, **, p<0.01, *, p<0.01 (unpaired Student's t-test on dCt values with Bonferroni's correction for multiple comparisons). D) Characterization of

Suppl. Fig.VI Permeability agents promote dissociation of perivascular macrophages.

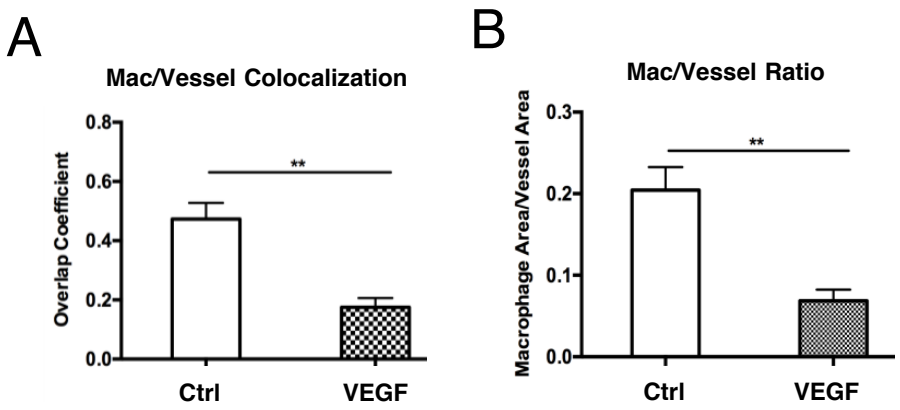

A) Quantification of macrophage and vessel co-localization using confocal images of mesenteric vessels in adeno-VEGF treated versus control animals, injected with empty adenoviral particles at similar titers. n= 3-4. **, $p<0.01$ (unpaired Student's t-test). B) Quantification of macrophage versus vessel by the occupied area. n= 3-4. **, $p<0.01$ (unpaired Student's t-test).